

# Higher partial waves in femtoscopy

Koichi Murase<sup>a,b</sup>, Tetsuo Hyodo<sup>a,b</sup>

<sup>a</sup>*Department of Physics, Tokyo Metropolitan University, 1-1  
Minami-Osawa, Hachioji, 192-0397, Tokyo, Japan*

<sup>b</sup>*RIKEN Interdisciplinary Theoretical and Mathematical Science Program  
(iTHEMS), 2-1 Hirosawa, Wako, 351-0198, Saitama, Japan*

---

## Abstract

Femtoscopy is recently gaining more attention as a new approach complementary to scattering experiments for constraining hadron-hadron interactions. We discuss the effect of higher partial waves on the two-particle correlation function, which has been neglected in traditional formulae used in the femtoscopy analyses. We consider the partial-wave expansion of the wave function in the Koonin–Pratt formula to give the correction to the correlation function by a sum of the contributions from each partial wave. We also generalize the Lednický–Lyuboshitz formula, which was originally derived for the  $s$ -wave interaction, for higher partial waves. We find a compact representation of the generalized Lednický–Lyuboshitz formula given by the backward scattering amplitude  $f(\theta = \pi)$  and the Fourier–Laplace transform of the relative source function, which gives an insight into the structure of the Lednický–Lyuboshitz formula and its relation to the optical theorem. We numerically demonstrate the significance of higher partial waves with resonances using the square potential well. Also, the generalized Lednický–Lyuboshitz formula turned out to be broken for higher partial waves, which suggests the importance of the centrifugal force with the higher partial waves.

*Keywords:* femtoscopy, higher partial wave, relativistic heavy-ion collisions, hadronic interaction

*PACS:* 25.75.Gz

---

## 1. Introduction

Recently, femtoscopy in high-energy nuclear collisions has been gathering attention as a new approach to hadron-hadron interaction [1–4]. Femtoscopy

allows us to access information about the particle source size and the wave function through the two-particle correlation function, which is actively measured in experiments recently [5–21]. The two-particle correlation function for a pair of particle species 1 and 2 is defined as

$$C_{12}(\mathbf{p}_1, \mathbf{p}_2) = C_{12}(\mathbf{q}, \mathbf{P}) = \frac{E_1 E_2 \frac{dN_{12}}{d\mathbf{p}_1 d\mathbf{p}_2}}{E_1 \frac{dN_1}{d\mathbf{p}_1} E_2 \frac{dN_2}{d\mathbf{p}_2}}, \quad (1)$$

where  $\mathbf{p}_1$  and  $\mathbf{p}_2$  are the momenta of the particles, and  $E_1 = E_1(\mathbf{p}_1)$  and  $E_2 = E_2(\mathbf{p}_2)$  are the corresponding energies. The momentum spectra of the particles are given by  $dN_1/d\mathbf{p}_1$  and  $dN_2/d\mathbf{p}_2$ . The pair distribution  $dN_{12}/d\mathbf{p}_1 d\mathbf{p}_2$  denotes the probability density that we find particles 1 and 2, with their respective momenta being  $\mathbf{p}_1$  and  $\mathbf{p}_2$ , simultaneously in a single event. The correlation function  $C_{12}$  is also written as a function of the relative and total momenta of the two-particle system,  $\mathbf{q}$  and  $\mathbf{P}$ , instead of  $\mathbf{p}_1$  and  $\mathbf{p}_2$ . In practice, the correlation function can be averaged for  $\mathbf{P}$  with a specific frame choice to define  $C_{12}(\mathbf{q})$ .

A perfect description of the correlation function in the high-energy nuclear collisions would require a theoretical understanding of dynamical particle production in the complicated processes of the collision reactions. Instead, based on a number of assumptions, the Koonin–Pratt (KP) [22–24] and Lednický–Lyuboshitz (LL) [25] formulae give useful expressions that calculate the two-particle correlation function in terms of the source function,  $S(\mathbf{r})$ , and the wave function,  $\varphi_{\mathbf{q}}^{(-)}(\mathbf{r})$ , with  $\mathbf{r}$  being the relative coordinates of the emission points of the two particles. Those formulae have proven their convenience and power in analyzing the correlation function in existing femtoscopy studies. However, as the experimental data for various particle pairs are becoming available with better statistics, precise and systematic determination of the hadronic interactions based on a realistic setup is gaining more importance. Some of the assumptions so far we relied upon may not be compatible with a realistic setup. It is important to revisit each assumption and consider its role.

In this study, we focus on the assumption of the  $s$ -wave interaction (i.e., the interaction for the orbital angular momentum  $l = 0$ ) used in the LL formula, where the contributions from  $p$ - and  $d$ -waves are neglected for simplicity. In general, the correlation function includes contributions from all

partial waves. The effect of higher partial waves is expected to be particularly significant in the presence of resonances of higher partial waves. For example, a peak around  $|\mathbf{q}| \simeq 240$  MeV observed in the  $K$ - $p$  correlation [10] is attributed to the  $d$ -wave resonance  $\Lambda(1520)$ . This peak in the correlation function has been attempted to be fit by a Breit–Wigner function [26] on top of the  $s$ -wave contribution, but its underlying justification and validity are not obvious. Recent ALICE results for the  $\Lambda$ - $K^-$  correlation [20] also show peaks associated with higher partial waves, such as the  $\Omega$  peak at  $|\mathbf{q}| \simeq 210.7$  MeV for the  $p$  wave and the  $\Xi(1820)$  peak at  $|\mathbf{q}| \simeq 398.9$  MeV for the  $d$  wave. In this study, we try to extend the KP and LL formula to include the contributions from higher partial waves and examine their properties. We assume  $\hbar = c = 1$  and  $\hbar c = 197.32$  MeV fm throughout this paper.

## 2. Koonin–Pratt and Lednický–Lyuboshitz formulae

We assume the KP formula [22, 23] as a starting point of this study and also consider the extension of the LL formula [25]. In this section, we overview the KP and LL formulae, which are widely used in femtoscopy to analyze the  $s$ -wave interaction.

The KP formula is based on a picture in which the two particles at the positions  $\mathbf{r}_1$  and  $\mathbf{r}_2$  are isolated from the rest of the system at an emission time and interact with each other as a two-body isolated system until the two-particle distance becomes sufficiently large. With an additional approximation<sup>1</sup> that the relative momentum  $\mathbf{q}_{\text{emit}}$  at emission can be replaced with the final momentum  $\mathbf{q}$ , the KP formula gives the two-particle correlation function with the integral:

$$C(\mathbf{q}) = \int d^3\mathbf{r} S_{12}(\mathbf{r}, \mathbf{q}) |\varphi_{\mathbf{q}}^{(-)}(\mathbf{r})|^2, \quad (2)$$

where  $\mathbf{r} = \mathbf{r}_1 - \mathbf{r}_2$  is the relative coordinates of the emission points  $\mathbf{r}_1$  and  $\mathbf{r}_2$ .

The relative source function  $S_{12}(\mathbf{r}, \mathbf{q})$ , with the normalization  $\int_0^\infty d^3\mathbf{r} S_{12}(\mathbf{r}, \mathbf{q}) = 1$ , gives the distribution of the relative positions  $\mathbf{r}$  of the particle pairs with

---

<sup>1</sup>This is typically justified by using the on-shell approximation, where the particles are assumed to be emitted in on-shell states, or the smoothness approximation, where the source function evaluated at  $\mathbf{q}_{\text{emit}}$  is assumed to be close to the one at  $\mathbf{q}$ .

the relative momentum  $\mathbf{q}$ . The dependence of  $S_{12}(\mathbf{r}, \mathbf{q})$  on  $\mathbf{q}$  is usually assumed to be negligible, and the relative source function is simply denoted as  $S(\mathbf{r}) := S_{12}(\mathbf{r}, \mathbf{q})$ .

The relative wave function  $\varphi_{\mathbf{q}}^{(-)}(\mathbf{r})$  represents the amplitude of finding the relative position of the two emission points at  $\mathbf{r}$  when the final relative momentum of the two particles is known to be  $\mathbf{q}$ . The wave function  $\varphi_{\mathbf{q}}^{(-)}(\mathbf{r})$  can be obtained by solving the Schrödinger equation under the boundary condition matching the outgoing wave with the plane wave of the asymptotic momentum  $\mathbf{q}$  at  $|\mathbf{r}| \rightarrow \infty$ . This is the opposite of the standard two-body scattering problem, where the incoming wave is normalized as a plane wave. The solution is related to the scattering wave function in the two-body scattering problem by the complex conjugate:  $\varphi_{\mathbf{q}}^{(-)}(\mathbf{r}) = [\varphi_{\mathbf{q}}(-\mathbf{r})]^*$ . In the following discussion, we consider the scattering wave function  $\varphi_{\mathbf{q}}(\mathbf{r})$  instead of  $\varphi_{\mathbf{q}}^{(-)}(\mathbf{r})$  to utilize the standard language in scattering. We consider the non-relativistic case and assume a short-range local potential in the Schrödinger equation:

$$\left[ -\frac{1}{2\mu} \nabla^2 + V(\mathbf{r}) \right] \varphi_{\mathbf{q}}(\mathbf{r}) = E_{\mathbf{q}} \varphi_{\mathbf{q}}(\mathbf{r}), \quad (3)$$

where  $\mu$  is the reduced mass of the two-body system, and the energy is specified by the asymptotic momentum:  $E_{\mathbf{q}} = q^2/(2\mu)$ . The boundary condition is given by

$$\varphi_{\mathbf{q}}(\mathbf{r}) = e^{iqz} + \frac{f(q, \theta)}{r} e^{iqr} + \mathcal{O}\left(\frac{1}{r^2}\right), \quad (r \rightarrow \infty), \quad (4)$$

where the  $z$ -axis is taken to be the direction of the relative momentum  $\mathbf{q}$ , and the polar angle  $\theta$  is the angle between the vectors,  $\mathbf{r}$  and  $\mathbf{q}$ . The function  $f(q, \theta)$  is an undetermined function of  $q$  and  $\theta$ . We here do not consider the symmetrization and antisymmetrization associated with the identical two bosons and fermions; the following discussion is only applicable to the non-identical particle pairs.

In the analyses for the  $s$ -wave interaction, we assume that only the  $s$ -wave part of the wave function is modified by the interaction, and the rest is kept to be that of the plane wave. In this case, the wave function is written as

$$\varphi_{\mathbf{q}}(\mathbf{r}) = e^{iqz} - j_0(qr) + R_0(r), \quad (5)$$

where  $j_0(qr)$  is the spherical Bessel function of the first kind, and  $R_0(r)$  is the radial wave function of the  $s$  wave<sup>2</sup>. The first two terms represent the plane wave without the  $s$ -wave component. If the source function is spherical,  $S(\mathbf{r}) = S(|\mathbf{r}|)$ , applying Eq. (5) to Eq. (2), we obtain an expression of the correlation function [2] as

$$C(q) = 1 + \int_0^\infty dr 4\pi r^2 S(r) [|R_0(r)|^2 - |j_0(qr)|^2]. \quad (6)$$

This expression shows that the deviation of the correlation function from unity is interpreted as the correction of the  $s$ -wave change from  $|j_0(qr)|^2$  to  $|R_0(r)|^2$ .

The Lednický–Lyuboshitz (LL) formula is another useful expression giving an explicit form of the correlation function, which is based on the KP formula with additional assumptions. In the LL formula, the  $s$ -wave function in the entire  $r$  region is replaced with the asymptotic form at  $r \rightarrow \infty$ ,

$$R_0^{\text{asy}}(r) = \frac{e^{i\delta_0(q)}}{qr} \sin[qr + \delta_0(q)], \quad (7)$$

determined by the phase shift  $\delta_0(q)$ . With the additional approximation that the source function is written in the spherical Gaussian form,

$$S(r) = \frac{1}{(4\pi R^2)^{3/2}} \exp\left(-\frac{r^2}{4R^2}\right), \quad (8)$$

the correlation function is given by

$$C_{\text{LL}}(q) = 1 + \frac{F_3(r_{\text{eff}}/R)}{2R^2} |f_0(q)|^2 + \frac{2F_1(2qR)}{\sqrt{\pi}R} \Re f_0(q) - \frac{F_2(2qR)}{R} \Im f_0(q), \quad (9)$$

where  $F_1(x) = \int_0^x dt \exp(t^2 - x^2)/x$ ,  $F_2(x) = (1 - e^{-x^2})/x$ , and  $F_3(x) = 1 - x/(2\sqrt{\pi})$ . The  $s$ -wave amplitude  $f_0$ <sup>3</sup> is related to the phase shift as  $f_0(q) = (e^{2i\delta_0(q)} - 1)/(2iq)$ . The second term of  $F_3(r_{\text{eff}}/R)$  is called the effective range correction and is introduced to partially compensate the approximation error by  $R_0^{\text{asy}}(r)$ :

$$\int dr 4\pi r^2 S(r) [|R_0(r)|^2 - |R_0^{\text{asy}}(r)|^2] \simeq -\frac{r_{\text{eff}}}{4\sqrt{\pi}R^3} |f_0(q)|^2, \quad (10)$$

where  $r_{\text{eff}} = (d/dq)^2 f_0(q)^{-1}|_{q=0}$  is the effective range.

---

<sup>2</sup>See Eq. (11) for an explicit definition of  $R_0(r)$ .

<sup>3</sup>See Eq. (18) for an explicit definition of  $f_0 = f_0(q)$ .

### 3. Higher partial waves

In this section, we extend the existing formulae for the correlation function with the  $s$ -wave correction to the general case with all partial waves. We first consider the generalization of the spherical-source KP formula (6) and the LL formula (9) in Secs. 3.1 and 3.2, respectively. We also discuss the structure of the LL formula in Sec. 3.3.

#### 3.1. KP formula with spherical source and higher partial waves

To extend the analysis for the general case where all the partial waves contribute, we may fully expand the wave function  $\varphi_{\mathbf{q}}(\mathbf{r})$  in partial waves:

$$\varphi_{\mathbf{q}}(r, \theta) = \sum_{l=0}^{\infty} (2l+1) i^l R_l(r) P_l(\cos \theta), \quad (11)$$

where  $P_l(\cos \theta) \propto Y_l^0(\theta, \phi)$  are the Legendre polynomials. It is noted that  $\varphi_{\mathbf{q}}$  is independent of the azimuthal angle  $\phi$  due to the symmetry in the potential and the boundary condition, so  $\varphi_{\mathbf{q}}(\mathbf{r})$  does not have the components  $Y_l^m(\theta, \phi)$  ( $m \neq 0$ ). A set of the radial wave functions  $\{R_l(r)\}_l$  for partial waves specifies a total wave function. For example, a plane wave  $\varphi_{\mathbf{q}} = e^{iqz}$  is specified by the spherical Bessel functions of the first kind,  $R_l(r) = j_l(qr)$ , as is known in the Rayleigh expansion. In the general case, the wave function is obtained as the solution to the Schrödinger equation. In the case of the central force  $V(r) = V(|\mathbf{r}_1 - \mathbf{r}_2|)$ , the partial wave function for each  $l$  can be solved independently:

$$\left[ -\frac{\partial^2}{\partial r^2} - \frac{2}{r} \frac{\partial}{\partial r} + \frac{l(l+1)}{r^2} + 2\mu V(r) \right] R_l(r) = q^2 R_l(r). \quad (12)$$

With the spherical source  $S(r)$ , we can apply Eq. (11) to Eq. (2) to obtain the correlation function in terms of  $S(r)$  and  $R_l(r)$ :

$$\begin{aligned} C(q) &= \sum_{l,l'=0}^{\infty} (2l+1)(2l'+1) \int d^3 \mathbf{r} S(r) i^{l'-l} R_l^*(r) R_{l'}(r) P_l(\cos \theta) P_{l'}(\cos \theta) \\ &= \sum_{l=0}^{\infty} (2l+1) \int dr 4\pi r^2 S(r) |R_l(r)|^2, \end{aligned} \quad (13)$$

where we used the orthogonality of the Legendre polynomials to eliminate one summation for the angular momentum  $l'$ . We note that when the source

function is not spherical, all the pairs of the partial waves of different  $l \neq l'$  interfere, and the correlation function cannot be written by a simple summation for  $l$ . Equation (13) gives the following relation for the plane wave,  $\varphi_{\mathbf{q}}(\mathbf{r}) = e^{iqz}$ :

$$1 = \sum_{l=0}^{\infty} (2l+1) \int dr 4\pi r^2 S(r) |j_l(qr)|^2, \quad (14)$$

where the unity on the left-hand side is directly obtained by the KP formula (2).

Subtracting Eq. (14) from Eq. (13), we obtain the correlation function in terms of the corrections:

$$C(q) = 1 + \sum_{l=0}^{\infty} \Delta C_l(q), \quad (15)$$

where  $\Delta C_l(q)$  is the correction by the interaction in the  $l$ -th partial wave:

$$\Delta C_l(q) = (2l+1) \int dr 4\pi r^2 S(r) [|R_l(r)|^2 - |j_l(qr)|^2]. \quad (16)$$

In the conventional case where only the  $s$  wave is assumed to be modified, all the higher-wave contributions  $\Delta C_l(q)$  ( $l \geq 1$ ) vanish so that Eqs. (15) and (16) reproduce the expression (6) known for the  $s$  wave.

### 3.2. LL formula generalized for higher partial waves

In addition to the spherical source assumption, the traditional LL formula assumes the asymptotic form of the  $s$ -wave function for the entire spatial region. To extend the LL formula for higher partial waves, it is useful to first remind us of the two levels of the asymptotic form of the wave function. For a short-range interaction, one can roughly separate the space into three parts depending on the relative distance: Region I is the spatial region within the interaction range  $r < r_{\text{int}}$  where both the potential interaction and the centrifugal force play roles. Region II is the intermediate region where the potential is negligible but the centrifugal force is still effective. Region III is the region where both the potential interaction and the centrifugal force are negligible when considering the wave-function form. The wave function in each region is given as the solution to the Schrödinger equation with the corresponding approximation. In Region I, the full Schrödinger equation (12)

needs to be solved. The solution there depends on the explicit form of the potential  $V(r)$ . The asymptotic form of the wave function in Region II is obtained by dropping the potential term  $V(r)$  and solving Eq. (12) with only the first three terms on the left-hand side. The solution is written by a linear combination of the spherical Hankel functions  $h_l(qr)$  and  $h_l^*(qr)$ :

$$R_l(r) \approx R_l^{\text{II}}(r) = \left[ \frac{1}{2} + iqf_l(q) \right] h_l(qr) + \frac{1}{2} h_l^*(qr), \quad (17)$$

where  $f_l$  is the partial-wave amplitude defined by the expansion of the scattering amplitude  $f(q, \theta)$ :

$$f(q, \theta) = \sum_{l=0}^{\infty} (2l+1) P_l(\cos \theta) f_l(q). \quad (18)$$

In this region, the potential information is rendered in the partial amplitudes  $f_l(q) = (e^{2i\delta_l(q)} - 1)/(2iq)$  written by the phase shifts  $\delta_l(q)$ , which are determined by the boundary condition with Region I. In Region III, the asymptotic wave function is solved with the first two terms on the left-hand side of Eq. (12), and the solution takes the form:

$$R_l(r) \approx R_l^{\text{III}}(r) = \frac{1}{i^l} \frac{1}{iqr} \left\{ \left[ \frac{1}{2} + iqf_l(q) \right] e^{iqr} - \frac{1}{2} (-1)^l e^{-iqr} \right\}. \quad (19)$$

In the case of the  $s$ -wave interaction, the wave functions in Regions II and III are the same  $R_0^{\text{II}}(r) = R_0^{\text{III}}(r)$  because the centrifugal potential  $l(l+1)/r^2$  vanishes for  $l = 0$ . A natural extension of the assumption of the asymptotic wave function (7) to an arbitrary angular momentum would be to use the asymptotic form  $R_l^{\text{II}}(r)$  or  $R_l^{\text{III}}(r)$ . However, approximation of the wave function by  $R_l^{\text{II}}(r)$  causes divergence of the correlation function with  $\delta_l \neq 0$  and  $S(0) \neq 0$  because the asymptotic wave function  $R_l^{\text{II}}(r)$  behaves as  $\sim 1/r^{l+1}$  near the origin.

Instead, we here consider  $R_l^{\text{III}}(r)$  for the wave function. Substituting Eq. (19) for Eq. (13), we obtain

$$C(q) = \frac{4\pi}{q^2} \int dr S(r) \sum_{l=0}^{\infty} (2l+1) \left\{ 1 - (-1)^{l+1} \Re \left[ \left( \frac{1}{2} + iqf_l \right) e^{2iqr} \right] \right\}. \quad (20)$$

In obtaining the above formula, the probability conservation<sup>4</sup> was used:

$$\frac{\mu}{q} \int j_r(r, \theta, \phi) r^2 d\Omega = \frac{4\pi}{q^2} \sum_{l=0}^{\infty} (2l+1) \left[ \left| \frac{1}{2} + iq f_l(q) \right|^2 - \left| \frac{1}{2} (-1)^l \right|^2 \right] = 0, \quad (21)$$

where  $d\Omega = d\phi d\cos\theta$ , and  $j_r = (1/\mu) \Im(\varphi_q^* \partial_r \varphi_q)$  is the  $r$ -component of the probability current with  $\varphi_q$  given by  $R_l^{\text{III}}(r)$  through Eq. (11). The  $r$  dependence of the asymptotic form cancel with the Jacobian  $r^2$  on the right-hand side. In the plain-wave case, the left-hand side of Eq. (20) becomes unity, while all  $f_l$  on the right-hand side vanish. Therefore, by subtracting the plain-wave case of Eq. (20) from itself, the correction to the correlation function is given by the terms proportional to  $f_l$ :

$$\begin{aligned} C(q) &= 1 + \frac{4\pi}{q} \sum_{l=0}^{\infty} (2l+1) (-1)^l \Im[f_l(q) \hat{S}(-2iq)] \\ &= 1 + \frac{4\pi}{q} \sum_{l=0}^{\infty} (2l+1) (-1)^l [\Im f_l(q) \Re \hat{S}(-2iq) + \Re f_l(q) \Im \hat{S}(-2iq)], \end{aligned} \quad (22)$$

where  $\hat{S}(-2iq) = \int_0^\infty dr S(r) e^{2iqr}$  is the Fourier–Laplace transform of the radial source function. In the case of the Gaussian relative source (8), the Fourier–Laplace transform is given by

$$\hat{S}(-2iq) = \frac{e^{-(2qR)^2}}{(4\pi)^{3/2} R^2} \left( \sqrt{\pi} + 2i \int_0^{2qR} dt e^{t^2} \right), \quad (23)$$

though Eq. (22) holds for any spherical source function. This gives a naive generalization of the LL formula with higher partial waves.

Let us confirm that Eq. (22) reproduces the original LL formula for  $s$  wave (9) except for the effective range correction. In the  $s$ -wave case, only the correction from  $l=0$  remains because  $f_l(q) = 0$  for  $l \geq 1$ . The original LL formula (9) has three correction terms proportional to  $|f_0(q)|^2$ ,  $\Re f_0(q)$ , and  $\Im f_0(q)$  unlike the generalized version (22), which has only two terms proportional to  $\Re f_l(q)$  and  $\Im f_l(q)$ . However, we notice that the first and third terms in the original LL formula can be combined using the optical

---

<sup>4</sup>Each term in the summation of Eq. (21) vanishes if the orbital angular momentum  $l$  is conserved, but it is unnecessary because we only use the total probability conservation here.

theorem for the partial amplitude,  $|f_0(q)|^2 = (1/q)\Im f_0(q)$ , so a simplified expression of the original LL formula is found:

$$C_{\text{LL}}(q) = 1 + \frac{F_4(2qR, r_{\text{eff}}/R)}{2qR^2} \Im f_0(q) + \frac{2F_1(2qR)}{\sqrt{\pi}R} \Re f_0(q), \quad (24)$$

where  $F_4(x, y) = e^{-x^2} - y/(2\sqrt{\pi})$ . The second argument of  $F_4(x, y)$  represents the effective range correction. It is easy to show that the coefficient functions in Eq. (24), excluding the effective range correction, match the real and imaginary parts of the Fourier–Laplace transform of the relative Gaussian source (23):

$$\frac{F_4(2qR, 0)}{2qR^2} = \frac{4\pi}{q} \Re \hat{S}(-2iq), \quad \frac{2F_1(2qR)}{\sqrt{\pi}R} = \frac{4\pi}{q} \Im \hat{S}(-2iq). \quad (25)$$

### 3.3. Generalized LL formula and optical theorem

Noticing  $(-1)^l = P_l(-1) = P_l(\cos \pi)$  and recalling Eq. (18), we may further simplify Eq. (22) by taking the sum over  $l$ :

$$C(q) = 1 + \frac{4\pi}{q} \Im [f(q, \theta = \pi) \hat{S}(-2iq)], \quad (26)$$

where  $f(q, \theta = \pi)$  is the backward scattering amplitude. This functional form is comparable to the optical theorem:

$$\sigma_{\text{tot}} = \frac{4\pi}{q} \Im f(q, \theta = 0), \quad (27)$$

where  $\sigma_{\text{tot}}$  is the total cross section, and  $f(q, \theta = 0)$  is the forward scattering amplitude.

The forward and backward amplitudes appearing in the optical theorem and the correlation function are related to the structure of the asymptotic form of the plane-wave expansion at the level of  $R_l^{\text{III}}(r)$ :

$$e^{iqz} = \frac{2}{iqr} [\delta(1 - \cos \theta) e^{iqr} - \delta(1 + \cos \theta) e^{-iqr}] + \mathcal{O}\left(\frac{1}{r^2}\right). \quad (28)$$

A convention of the Dirac delta function  $\delta(z)$  was chosen so that  $\int_0^\infty dz \delta(z)g(z) = g(0)/2$  with  $g(z)$  being an arbitrary function analytic at  $z = 0$ . The above expression can be obtained by retaining only the  $\mathcal{O}(1/r)$  contributions of  $R_l(r) = j_l(qr) \approx (1/qr) \sin(qr - l\pi/2)$  in the Rayleigh expansion (11) and

comparing them with the Legendre expansion of the delta functions. This asymptotic expression of the plane wave contains the two delta functions peaking at  $\cos \theta = \pm 1$  (i.e.,  $\theta = 0, \pi$ ), which suggests that the significance of forward and backward directions is already built in the structure of the plane wave.

In fact, both the optical theorem (27) and the generalized LL formula (26) can be easily derived by using Eq. (28). The scattering wave function can be written as

$$\varphi_{\mathbf{q}}(\mathbf{r}) = e^{iqz} + \frac{f(q, \theta)}{r} e^{iqr} = \frac{1}{iqr} [B(\theta) e^{iqr} - C(\theta) e^{-iqr}] + \mathcal{O}\left(\frac{1}{r^2}\right), \quad (29)$$

where

$$B(\theta) = 2\delta(1 - \cos \theta) + iqf(q, \theta), \quad C(\theta) = 2\delta(1 + \cos \theta). \quad (30)$$

The optical theorem is obtained by the balance of the probability fluxes of the outgoing and incoming waves:

$$\begin{aligned} 0 &= \int r^2 d\Omega \frac{1}{(qr)^2} [|B(\theta)|^2 - |C(\theta)|^2] \\ &= \int d\Omega \frac{1}{q^2} \{2\Re[2iqf(q, \theta)\delta(1 - \cos \theta)] + q^2|f(q, \theta)|^2\} \\ &= -\frac{4\pi}{q} \Im[f(q, \theta = 0)] + \sigma_{\text{tot}}, \end{aligned} \quad (31)$$

where the interference of the two terms in  $B(\theta)$  picks up the forward amplitude  $f(q, \theta = 0)$ . The correlation function is given by the KP formula:

$$\begin{aligned} C(q) &= \int_0^\infty r^2 dr S(r) \int d\Omega \frac{1}{(qr)^2} |B(\theta) e^{iqr} - C(\theta) e^{-iqr}|^2 \\ &= \int_0^\infty dr S(r) \int d\Omega \frac{1}{q^2} \{2|C(\theta)|^2 - 2\Re[B(\theta)C(\theta)^* e^{2iqr}]\}. \end{aligned} \quad (32)$$

By subtracting the plane-wave contribution, we obtain

$$\begin{aligned} C(q) &= 1 - \int_0^\infty dr S(r) \int d\Omega \frac{1}{q^2} 2\Re[2iqf(q, \theta)\delta(1 + \cos \theta)e^{2iqr}] \\ &= 1 + \frac{4\pi}{q} \int_0^\infty dr S(r) \Im[f(q, \theta)e^{2iqr}] \\ &= 1 + \frac{4\pi}{q} \Im[f(q, \theta)\hat{S}(-2iq)], \end{aligned} \quad (33)$$

where we observe that the interference of  $f(q, \theta)$  and  $C(\theta)$  picks up the backward amplitude  $f(q, \theta = \pi)$ .

## 4. Numerical results

For demonstration and examination of the formulae we obtained for the higher partial waves, we consider a square potential well:

$$V(r) = \begin{cases} -V_0, & (r < b), \\ 0, & (r > b), \end{cases} \quad (34)$$

with the depth  $V_0$  and the width  $b$  being the potential parameters.

### 4.1. Spherical-source KP formula with higher partial waves

We first consider the KP formula with the spherical source (15) and (16). Figure 1 shows the magnitudes of the corrections to the correlation function from different partial waves in the case of the Gaussian source (8). The potential parameters,  $V_0 = 50$  MeV and  $b = 1$  fm, are chosen to be weakly attractive so that no bound states appear. The other parameter is given in the figure caption.

At a lower relative momentum  $q$  of Fig. 1, we see that the higher orders of the partial waves are suppressed by orders of magnitude. This is because the wave function is asymptotically given by  $R_l(r) \approx j_l(qr) + f_l(q)h_l(qr)$ , where the effective range expansion of the partial amplitude implies the parametric dependence of  $f_l = q^{2l}/[-1/a_l + \mathcal{O}(q^2) - iq^{2l+1}] \sim q^{2l}$  at  $q \rightarrow 0$  for  $|a_l| < \infty$ . Therefore, the correction is expected to usually behave in the limit  $q \rightarrow 0$  as

$$\Delta C_l(q) \sim |R_l(r)|^2 - |j_l(qr)|^2 \sim f_l \sim q^{2l}. \quad (35)$$

This dependence is manifested in the bottom panel of Fig. 1, where the slope of each correction reads  $2l$  in the log-log plot at small  $q$ . This means that the contributions from the higher partial waves are usually negligible by orders of magnitude at small  $q$ . This is also consistent with the original paper of the LL formula [25], which concluded that the  $s$ -wave approximation works well for  $q \leq 50$  MeV within the 1% error.

However, the contributions from higher partial waves become comparable when the relative momentum  $q$  becomes larger. In particular, when the lower-order contributions of the partial waves crosses zero, the contribution

of higher partial waves can be larger than the lower orders. For example, the spike around  $q \simeq 200$  MeV in the  $l = 0$  case on the top panel of Fig. 1 indicates that the  $s$ -wave correction  $\Delta C_0(q)$  crosses zero. In this case, the  $p$  wave ( $l = 1$ ) has a larger contribution at larger  $q$ .

It should be noted that the detailed behavior largely depends on the potential and its parameters. In particular, when there are resonances of higher partial waves near the real axis in the  $q$  plane, the peaks associated with the resonances appear in the correlation function. Figure 2 shows the correlation function with deeper square potential well. The top and bottom panels show the results with  $V_0 = 300$  and 600 MeV, respectively. Unlike the shallow case of  $V_0 = 50$  MeV in Fig. (1), the red lines ( $l = 0$ ) are negative in both panels because of an  $s$ -wave bound state. We find significant peaks of the correlation function corrections by the  $p$  wave ( $l = 1$ ) and the  $d$  wave ( $l = 2$ ) at  $q \simeq 90$  MeV on the top panel and  $q \simeq 190$  MeV on the bottom panel, respectively, and the magnitude of the peaks are significantly larger than the magnitude of the  $s$ -wave ( $l = 0$ ) correction. In the case of  $V_0 = 300$  MeV, the  $p$ -wave contribution has almost the same magnitude as the  $s$ -wave contribution even at a low momentum  $q \simeq 50$  MeV. This tells us that the corrections of the higher partial waves can be more significant than the  $s$ -wave contribution, depending on the details of the potential.

#### 4.2. Generalized LL formula for higher partial waves

We next examine the generalized LL formula (22). While the partial wave contributions of the KP formula (16) are exact under the assumption of the spherical source, the generalized LL formula (22) uses an assumption that the wave function in the entire spatial region may be replaced by the  $\mathcal{O}(1/r)$  asymptotic form neglecting the centrifugal corrections. This assumption appears to be highly nontrivial to justify in the case of higher partial waves ( $l \geq 0$ ). Here, the generalized LL formula shall be compared to the exact spherical-source KP formula to examine whether it gives a reasonable approximation to the spherical-source KP formula.

Figure 3 compares the generalized LL formula to the partial wave contribution of the KP formula. Panels (a) and (b) correspond to different potential depths,  $V_0 = 100$  and 300 fm, respectively. We can first confirm that the generalized LL and KP formulae for the  $s$ -wave case ( $l = 0$ ), which are nothing but the traditional LL and KP formulae, are in good agreement with each other. It should be noted that the generalized LL formula does not include the effective range correction, which was present in the original

LL formula, so the slight differences may be partly explained by the effective range correction.

In the cases of higher partial waves ( $l \geq 0$ ), however, the generalized LL formula fails to reproduce the KP formula even qualitatively. In particular, the sign of the corrections are opposite for the odd  $l$  due to the  $(-1)^l$  factor in Eq. (22). This factor  $(-1)^l$  comes from the phase  $-l\pi/2$  in the asymptotic spherical Bessel function  $j_l(qr) \approx \sin(qr - l\pi/2)/(qr)$ , ( $r \rightarrow \infty$ ). The correction to the correlation function reflects the change of  $|R_l^{\text{III}}(r)|^2 \sim |\sin(qr - l\pi/2 + \delta_l)|/(qr)^2$  near the origin, where the source function  $S(r)$  has a support, by a finite  $\delta_l$ . Figure 4 depicts the effect of the phase shift on the asymptotic wave function of each angular momentum in a modestly attractive case ( $0 < \delta_l < \pi/2$ ). We notice that the magnitude of the wave function increases near the origin for even  $l$ , while it decreases for odd  $l$ . However, this behavior is unphysical. First, the wave function  $R_l^{\text{III}}(r) = \sin(qr - l\pi/2 + \delta_l)/(qr)$  diverges at the origin (except for very special values of the phase shift,  $\delta_l = l\pi/2 + n\pi$ ,  $n \in \mathbb{Z}$ ). This problem is already present with the assumption behind the traditional LL formula. More physically, the wave function near the origin should be suppressed by the centrifugal force as  $R_l(r) \approx r^l$ , ( $r \rightarrow 0$ ), which is not taken into account in the wave function of the LL formula.

This means that the generalized LL formula (22) gives the contribution of only a part of the wave function of the order  $\mathcal{O}(1/r)$  and misses an important part. Although it gives an insight into the structure of the LL formula as discussed in Sec. 3.3, it is not practically useful for higher partial waves ( $l \geq 1$ ) at all. Even for the traditional case for the  $s$  wave ( $l = 0$ ), the asymptotic wave function used in the formula appears to have an unphysical behavior near the origin. A typical usage of the LL formula is to relate the correlation function to the parameters of the effective range expansion, where the asymptotic wave function can be regarded as merely one model of the wave function parametrized by the phase shift or the parameters of the effective range expansion. In this sense, we can choose another more physical wave function as a reference model for an improved LL formula.

## 5. Summary

Femtoscopy in high-energy collisions gives a novel and complementary approach to the hadron interaction in combination with traditional scattering experiments. The understanding of the assumptions and applicability of

historical formulae used in femtoscopy is of great interest for future analyses for the precise determination of the hadron interactions. Important formulae widely used in the analyses include the spherical-source KP formula (6) [2] and the LL formula (9) [25], which assume that the two particles interact through only the  $s$  wave ( $l = 0$ ). However, it is nontrivial whether the higher partial waves ( $l \geq 1$ ) are negligible at all. In this study, we considered the contributions of the higher partial waves by extending the spherical-source KP formula (6) and the LL formula (9) assuming the KP formula (2).

We obtained the spherical-source KP formula with the contributions from all partial waves in Eqs. (15) and (16). They are summarized in the following form:

$$C(q) = 1 + \sum_{l=0}^{\infty} (2l+1) \int dr 4\pi r^2 S(r) [ |R_l(r)|^2 - |j_l(qr)|^2 ], \quad (36)$$

where the correlation function gets the contributions of partial waves as the sum of the contribution from each partial wave.

We also obtained the generalized version of the LL formula (22) (except for the effective range correction) by approximating the wave function with the  $\mathcal{O}(1/r)$  asymptotic form for the entire spatial region. Furthermore, the sum for the angular momentum  $l$  in Eq. (22) can be explicitly performed to obtain a more compact representation (26). These results can be summarized in the following formula:

$$\begin{aligned} C(q) &= 1 + \frac{4\pi}{q} \Im[f(q, \theta = \pi) \hat{S}(-2iq)] \\ &= 1 + \frac{4\pi}{q} \sum_{l=0}^{\infty} (2l+1)(-1)^l \Im[f_l(q) \hat{S}(-2iq)], \end{aligned} \quad (37)$$

where  $\hat{S}(-2iq)$  is the Fourier–Laplace transform of the relative source  $S(r)$ . This reproduces the traditional LL formula (9) for the  $s$ -wave case, where two of the three correction terms come from  $\Im f_0(q) \Re \hat{S}(-2iq)$  (except for the effective range correction), and the rest comes from  $\Re f_0(q) \Im \hat{S}(-2iq)$ . We also point out that the correction to the correlation function can be written by the backward scattering amplitude  $f(q, \theta = \pi)$ , and the structure is similar to the optical theorem. We showed that both the optical theorem and the correlation function with the LL formula stem from an asymptotic structure of the plane wave written by the forward and backward delta functions. In

particular, the nontrivial parts in both cases come from interference between the scattering amplitude  $f_l(q, \theta)$  and the delta functions in the plane wave.

The corrections by the higher partial waves based on the KP formula (16) were investigated for the square potential well by changing the depth  $V_0$ . In normal cases without resonances, the contribution of higher partial waves to the correlation function is suppressed by orders of magnitude at low momentum  $q$ , while it can be dominant at high  $q$  depending on the potential. With resonances in higher partial waves ( $l > 0$ ), the contribution of the higher partial wave can be more significant than the  $s$ -wave ( $l = 0$ ) contribution. The generalized LL formula (22) was also examined in comparison with the KP formula but turned out to fail for higher partial waves ( $l \geq 1$ ). This is due to an unphysical behavior of the asymptotic wave function applied to the interacting region  $r \approx 0$ . This suggests the necessity of an alternative wave-function form for an improved LL formula, which will be discussed in our forthcoming paper.

### Acknowledgement

The authors thank Asanosuke Jinno and Yuki Kamiya for useful discussions. The work has been supported by JSPS KAKENHI Grant Numbers JP23H05439 (K.M. and T.H.), JP23K13102 (K.M.), and JP22K03637 (T.H.).

### References

- [1] A. Ohnishi, Y. Hirata, Y. Nara, S. Shinmura, Y. Akaishi, Can we extract Lambda-Lambda interaction from two particle momentum correlation?, *Nucl. Phys. A* 670 (2000) 297–300. [arXiv:nucl-th/9903021](https://arxiv.org/abs/nucl-th/9903021), doi:10.1016/S0375-9474(00)00117-2.
- [2] K. Morita, T. Furumoto, A. Ohnishi,  $\Lambda\Lambda$  interaction from relativistic heavy-ion collisions, *Phys. Rev. C* 91 (2) (2015) 024916. [arXiv:1408.6682](https://arxiv.org/abs/1408.6682), doi:10.1103/PhysRevC.91.024916.
- [3] S. Cho, T. Hyodo, D. Jido, C. M. Ko, S. H. Lee, S. Maeda, K. Miyahara, K. Morita, M. Nielsen, A. Ohnishi, T. Sekihara, T. Song, S. Yasui, K. Yazaki, Exotic hadrons from heavy ion collisions, *Progress in Particle and Nuclear Physics* 95 (2017) 279–322. [arXiv:1702.00486](https://arxiv.org/abs/1702.00486), doi:<https://doi.org/10.1016/j.ppnp.2017.02.002>.

URL <https://www.sciencedirect.com/science/article/pii/S0146641017300182>

- [4] L. Fabbietti, V. Mantovani Sarti, O. Vazquez Doce, Study of the Strong Interaction Among Hadrons with Correlations at the LHC, *Ann. Rev. Nucl. Part. Sci.* 71 (2021) 377–402. [arXiv:2012.09806](https://arxiv.org/abs/2012.09806), doi:10.1146/annurev-nucl-102419-034438.
- [5] L. Adamczyk, et al.,  $\Lambda\bar{\Lambda}$  Correlation Function in Au+Au collisions at  $\sqrt{s_{NN}} = 200$  GeV, *Phys. Rev. Lett.* 114 (2) (2015) 022301. [arXiv:1408.4360](https://arxiv.org/abs/1408.4360), doi:10.1103/PhysRevLett.114.022301.
- [6] L. Adamczyk, et al., Measurement of Interaction between Antiprotons, *Nature* 527 (2015) 345–348. [arXiv:1507.07158](https://arxiv.org/abs/1507.07158), doi:10.1038/nature15724.
- [7] S. Acharya, et al., p-p, p- $\Lambda$  and  $\Lambda\bar{\Lambda}$  correlations studied via femtoscopy in pp reactions at  $\sqrt{s} = 7$  TeV, *Phys. Rev. C* 99 (2) (2019) 024001. [arXiv:1805.12455](https://arxiv.org/abs/1805.12455), doi:10.1103/PhysRevC.99.024001.
- [8] S. Acharya, et al., First Observation of an Attractive Interaction between a Proton and a Cascade Baryon, *Phys. Rev. Lett.* 123 (11) (2019) 112002. [arXiv:1904.12198](https://arxiv.org/abs/1904.12198), doi:10.1103/PhysRevLett.123.112002.
- [9] S. Acharya, et al., Investigation of the p- $\Sigma$ 0 interaction via femtoscopy in pp collisions, *Phys. Lett. B* 805 (2020) 135419. [arXiv:1910.14407](https://arxiv.org/abs/1910.14407), doi:10.1016/j.physletb.2020.135419.
- [10] S. Acharya, et al., Scattering studies with low-energy kaon-proton femtoscopy in proton-proton collisions at the LHC, *Phys. Rev. Lett.* 124 (9) (2020) 092301. [arXiv:1905.13470](https://arxiv.org/abs/1905.13470), doi:10.1103/PhysRevLett.124.092301.
- [11] S. Acharya, et al., Study of the  $\Lambda\bar{\Lambda}$  interaction with femtoscopy correlations in pp and p-Pb collisions at the LHC, *Phys. Lett. B* 797 (2019) 134822. [arXiv:1905.07209](https://arxiv.org/abs/1905.07209), doi:10.1016/j.physletb.2019.134822.
- [12] A. Collaboration, et al., Unveiling the strong interaction among hadrons at the LHC, *Nature* 588 (2020) 232–238, [Erratum: *Nature* 590, E13 (2021)]. [arXiv:2005.11495](https://arxiv.org/abs/2005.11495), doi:10.1038/s41586-020-3001-6.

- [13] S. Acharya, et al., Exploring the  $\Lambda$ – $\Sigma$  coupled system with high precision correlation techniques at the LHC, *Phys. Lett. B* 833 (2022) 137272. [arXiv:2104.04427](https://arxiv.org/abs/2104.04427), doi:10.1016/j.physletb.2022.137272.
- [14] S. Acharya, et al., Investigating the role of strangeness in baryon–antibaryon annihilation at the LHC, *Phys. Lett. B* 829 (2022) 137060. [arXiv:2105.05190](https://arxiv.org/abs/2105.05190), doi:10.1016/j.physletb.2022.137060.
- [15] S. Acharya, et al., Experimental Evidence for an Attractive  $p$ – $\phi$  Interaction, *Phys. Rev. Lett.* 127 (17) (2021) 172301. [arXiv:2105.05578](https://arxiv.org/abs/2105.05578), doi:10.1103/PhysRevLett.127.172301.
- [16] S. Acharya, et al., Kaon–proton strong interaction at low relative momentum via femtoscopy in  $\text{Pb}$ – $\text{Pb}$  collisions at the LHC, *Phys. Lett. B* 822 (2021) 136708. [arXiv:2105.05683](https://arxiv.org/abs/2105.05683), doi:10.1016/j.physletb.2021.136708.
- [17] S. Acharya, et al., First measurement of the  $\Lambda$ – $\Xi$  interaction in proton–proton collisions at the LHC, *Phys. Lett. B* 844 (2023) 137223. [arXiv:2204.10258](https://arxiv.org/abs/2204.10258), doi:10.1016/j.physletb.2022.137223.
- [18] S. Acharya, et al., First study of the two-body scattering involving charm hadrons, *Phys. Rev. D* 106 (5) (2022) 052010. [arXiv:2201.05352](https://arxiv.org/abs/2201.05352), doi:10.1103/PhysRevD.106.052010.
- [19] S. Acharya, et al., Constraining the  $\bar{K}\Lambda$  coupled channel dynamics using femtoscopic correlations at the LHC, *Eur. Phys. J. C* 83 (4) (2023) 340. [arXiv:2205.15176](https://arxiv.org/abs/2205.15176), doi:10.1140/epjc/s10052-023-11476-0.
- [20] S. Acharya, et al., Accessing the strong interaction between  $\Lambda$  baryons and charged kaons with the femtoscopy technique at the LHC, *Phys. Lett. B* 845 (2023) 138145. [arXiv:2305.19093](https://arxiv.org/abs/2305.19093), doi:10.1016/j.physletb.2023.138145.
- [21] S. Acharya, et al., Studying the interaction between charm and light-flavor mesons, *Phys. Rev. D* 110 (3) (2024) 032004. [arXiv:2401.13541](https://arxiv.org/abs/2401.13541), doi:10.1103/PhysRevD.110.032004.
- [22] S. E. Koonin, Proton Pictures of High-Energy Nuclear Collisions, *Phys. Lett. B* 70 (1977) 43–47. doi:10.1016/0370-2693(77)90340-9.

- [23] S. Pratt, Pion Interferometry for Exploding Sources, *Phys. Rev. Lett.* 53 (1984) 1219–1221. [doi:10.1103/PhysRevLett.53.1219](https://doi.org/10.1103/PhysRevLett.53.1219).
- [24] W. Bauer, C. K. Gelbke, S. Pratt, Hadronic interferometry in heavy ion collisions, *Ann. Rev. Nucl. Part. Sci.* 42 (1992) 77–100. [doi:10.1146/annurev.ns.42.120192.000453](https://doi.org/10.1146/annurev.ns.42.120192.000453).
- [25] R. Lednický, V. L. Lyuboshits, Final State Interaction Effect on Pairing Correlations Between Particles with Small Relative Momenta, *Yad. Fiz.* 35 (1981) 1316–1330.
- [26] Y. Kamiya, T. Hyodo, K. Morita, A. Ohnishi, W. Weise,  $K^-p$  Correlation Function from High-Energy Nuclear Collisions and Chiral SU(3) Dynamics, *Phys. Rev. Lett.* 124 (13) (2020) 132501. [arXiv:1911.01041](https://arxiv.org/abs/1911.01041), [doi:10.1103/PhysRevLett.124.132501](https://doi.org/10.1103/PhysRevLett.124.132501).

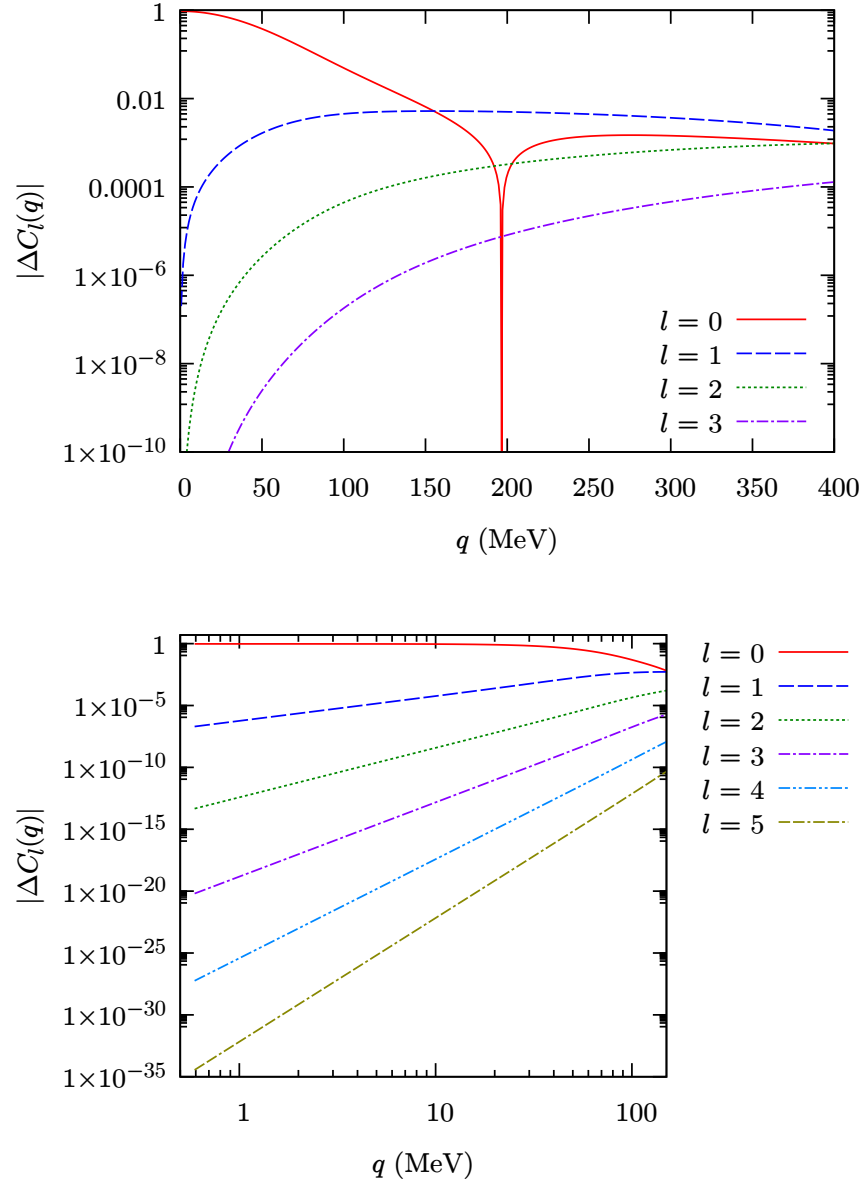


Figure 1: The magnitudes of the corrections (16) to the correlation function from each partial wave. The reduced mass, the potential parameters, and the source size are chosen to be  $\mu = 600$  MeV,  $V_0 = 50$  MeV,  $b = 1$  fm, and  $R = 2$  fm. The vertical axis shows the absolute value of the correction of each partial wave on a logarithmic scale. The horizontal axis indicates the relative momentum  $q$ . The top panel shows the behavior in a wide range of  $q$ , while the bottom panel shows the behavior at small  $q$  with the logarithmic scale in the horizontal axis.

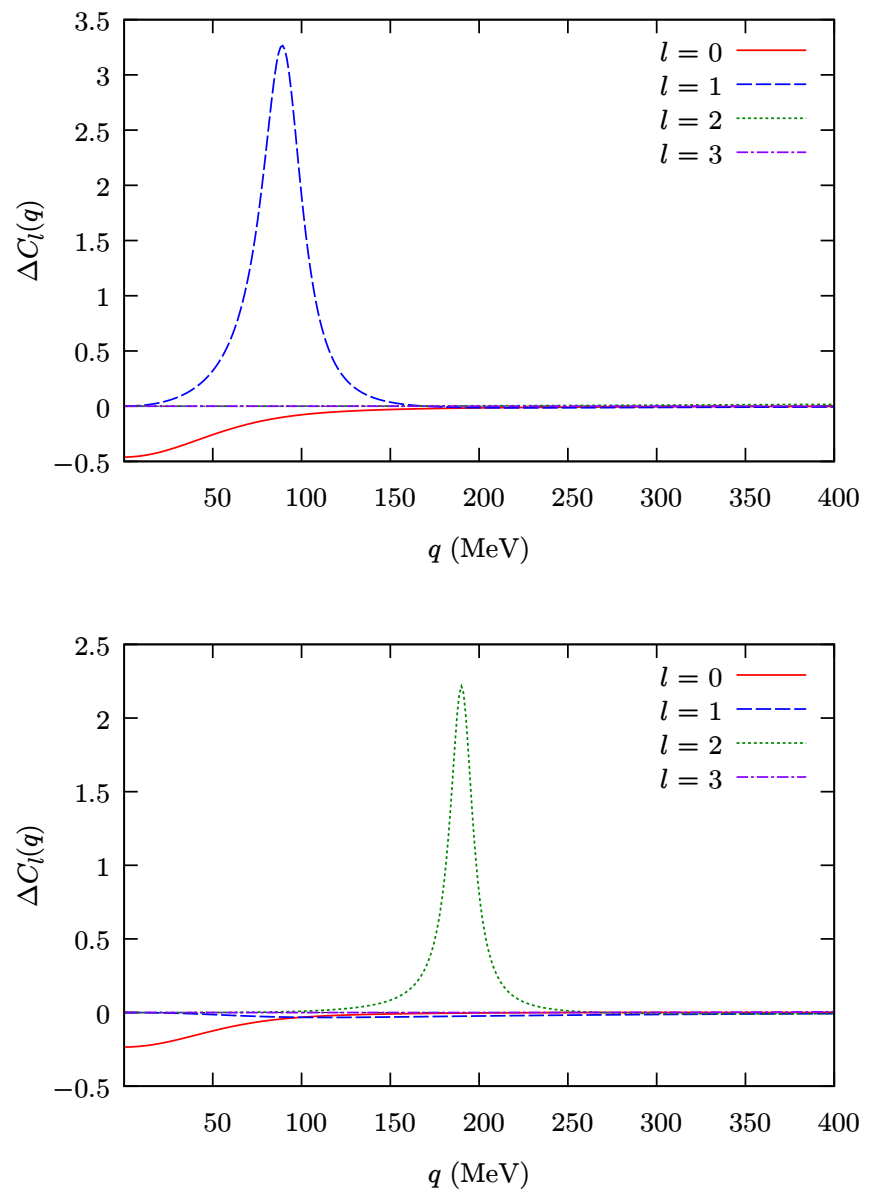


Figure 2: The same as Fig. 2 but with deeper potentials:  $V_0 = 300$  and 600 MeV for the top and bottom panels, respectively.

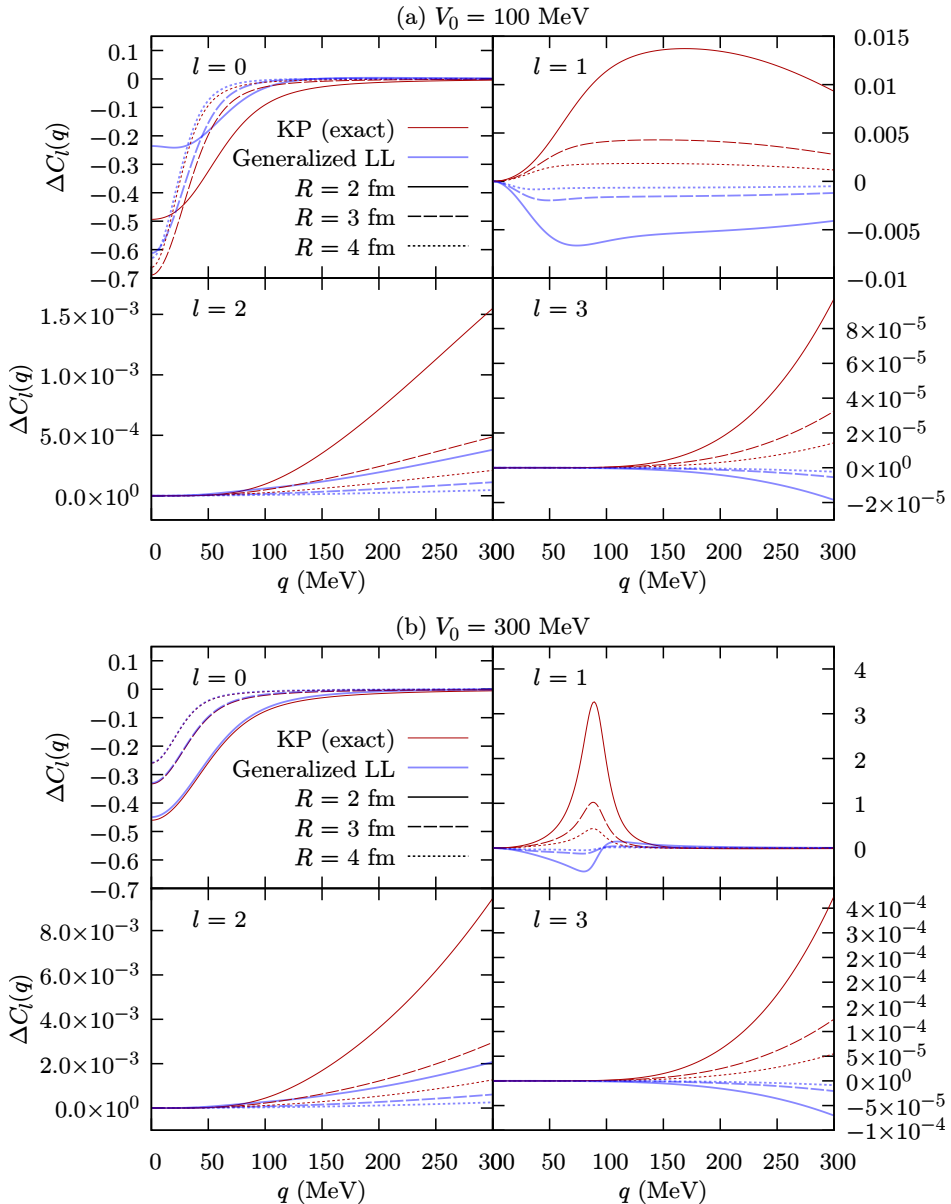


Figure 3: Comparison of the generalized LL formula to the corresponding correction in the KP formula with the direct integration. Panels (a) and (b) panel show the results with  $V_0 = 100$  and 300 MeV, respectively. In each panel, the results for different angular momenta  $l = 0, 1, 2, 3$  are shown from the top left to the bottom right. The thin red and bold blue lines correspond to the KP and the generalized LL formulae, respectively. The solid, dashed, and dotted lines correspond to different source sizes  $R = 2, 3$ , and 4 fm. The other parameters are the same as in Fig. 1.

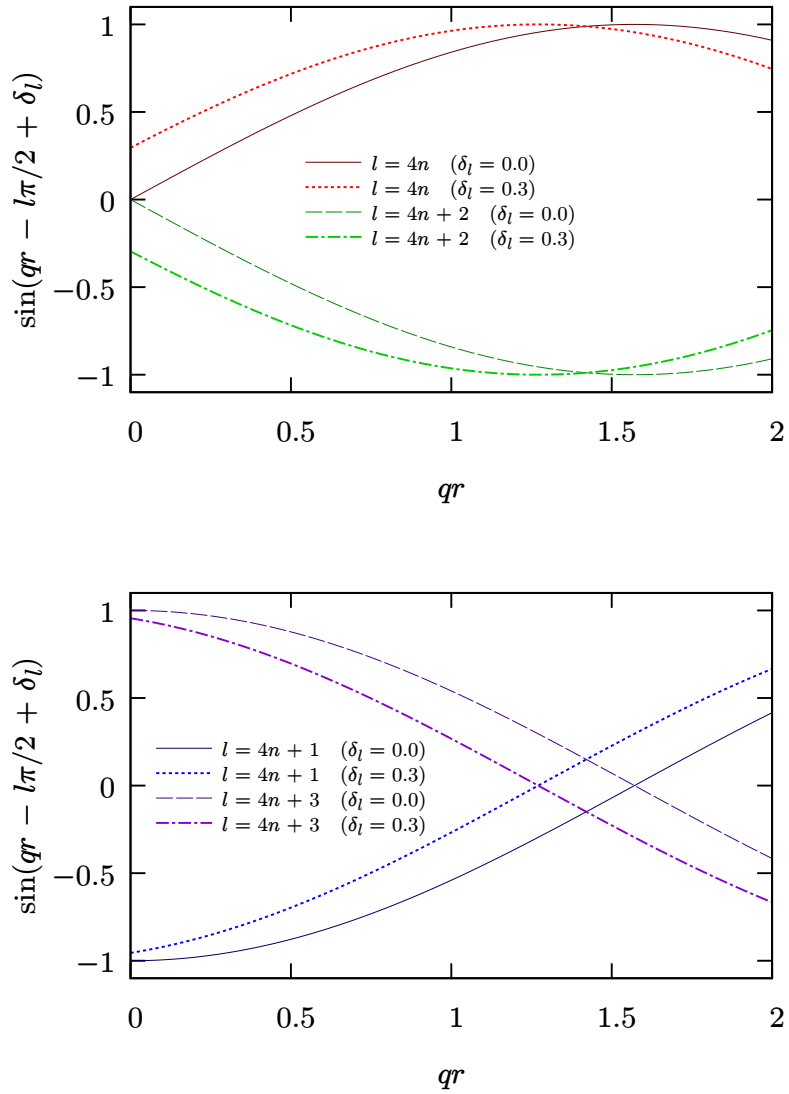


Figure 4: Phase shift effects on the asymptotic partial wave functions. The top and bottom panels show the cases of odd and even  $l$ 's, respectively.